MONITORING ALTAIR'S FAR-ULTRAVIOLET EMISSION LINES FOR VARIABILITY OVER A STELLAR ROTATION PERIOD

S. Redfield[1] and J. L. Linsky[2]

[1]McDonald Observatory, University of Texas, Austin, TX 78712, USA
[2]JILA, University of Colorado and NIST, Boulder, CO 80309, USA

Abstract

Ultraviolet and X-ray observations show that high temperature plasma is present in the outer atmospheres of late-type dwarf stars including late A-type stars. Aside from the detection of coronae in late-A stars and the emission rates from these hot plasmas, we know very little about their structure and heating mechanisms. The *Far Ultraviolet Spectroscopic Explorer* (*FUSE*) has the unique capability to provide new information on both of these topics. *FUSE* can Doppler image rapidly rotating late-A stars in lines of C III and O VI. If the hot plasma is located primarily in bright active regions, the shapes of these emission lines will change with time as the active regions rotate across the stellar disk. The existence of active regions will tell us unambiguously that the hot plasma is magnetically confined and magnetically heated, rather than heated by acoustic waves. Existing *FUSE* spectra of Altair show that the O VI and C III emission lines have a horned appearance, indicating that emission near the limbs can be resolved due to the rapid rotation of the star. We present a new long (27 ksec) *FUSE* observation of Altair, and explore emission line variability over a stellar rotation period.

Key words: line: profiles – stars: atmospheres – stars: early-type – stars: individual (Altair) – stars: rotation – ultraviolet: stars

1. Far Ultraviolet Spectra of Altair

The full far-ultraviolet (FUV) spectrum (900-1200 Å) of Altair (α Aql) obtained by the *Far Ultraviolet Spectroscopic Explorer*[1] (*FUSE*) is shown in Figure 1. The FUV is a unique wavelength region for observing A stars, because only at these short wavelengths do stellar emission lines dominate over the stellar continuum, which is clearly rising at the longer wavelengths. The shaded bands indicate spectral regions that may be contaminated by terrestrial airglow lines, such as OI and HI Lyman lines. Stellar emission lines are identified, including the very strong lines of C III λ977 and O VI $\lambda\lambda$1031, 1036. The mere presence of these hot transition region lines in A stars is also of interest. Altair is near the boundary where shallow dynamo-driven convection zones appear, along with coronal and transition region activity, producing emission in X-rays and in lines such as C III and O VI (Simon et al. 2002).

The "horned" or "double-peaked" emission line shape of the transition region lines of Altair are unique among observed late-type stars. Redfield et al. (2002, 2003) surveyed late-type stars observed by *FUSE*, and only Altair showed this "horned" line profile. Altair's large rotational velocity ($v \sin i \sim 210$ km s^{-1}) Doppler shifts the various stellar rotational zones so that limb effects are clearly detected, even at the moderate resolution of *FUSE* ($R \sim 20{,}000$ or 15 km s^{-1}). The "horned" profile is a result of limb-brightening. As we move from the center of the star to its limb (from Doppler shifted emission at 0 to 210 km s^{-1}), optical depth unity is reached at shallower depths of the atmosphere (farther from the photosphere and closer to the corona). Photospheric emission in the optical, will therefore decrease as we sample cooler layers, leading to limb-darkening. However, coronal and transition region emission, such as the C III and O VI lines, will increase as we traverse more coronal layers, leading to limb-brightening. Limb-brightening in UV lines has been observed on the Sun (Doschek et al. 1975; Crane et al. 2004), and has a $1/\mu$ dependence, where $\mu = \cos\theta$ (Wilhelm et al. 1998).

Huenemoerder et al. (1993) observed an active G-star, FK Com, and detected He I D3 absorption lines in the optical that showed emission in the far wings, indicating limb-brightening. However, the He I D3 absorption profile is highly variable, due to the inhomogeneous source of coronal photons, that ionizes photospheric helium (Zirin 1975). Transition regions lines, such as C III and O VI, are more stable features, and therefore provide a better opportunity to detect distinct transitory structures in the emission line profile.

2. Heating Mechanisms & Limb-Brightened Lines

The presence of hot plasma in the outer atmospheres of stars at least as hot as $T_{\rm eff} = 8200$ K is undisputed by the presence of these transition region lines in the FUV (Simon et al. 2002). However, it is still unclear how this material is heated. Shocks driven by strong acoustic waves,

[1] Based on observations made with the NASA-CNES-CSA *Far Ultraviolet Spectroscopic Explorer*. *FUSE* is operated for NASA by the Johns Hopkins University under NASA contract NAS5-32985.

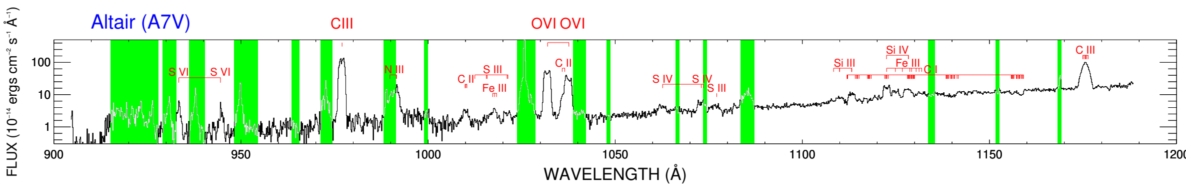

Figure 1. Full far-ultraviolet spectrum of Altair, observed by FUSE. The shaded bands indicate regions of possible terrestrial airglow contamination by O I and H I. Strong emission lines are labeled, and the rise of the continuum can be seen at the longest wavelengths. The strongest emission lines in this late-A star are C III λ977 and O VI λλ1031, 1036.

generated in the shallow convective zones of these A stars could be the prime heating source. On the other hand, many A stars have detected magnetic fields and localized chemical peculiarities associated with these fields (Hatzes 1996), so magnetic heating is also possible. By monitoring the Doppler-broadened transition region lines of Altair for variations, effectively "Doppler-imaging" the transition region of this star, we will be able to search for small-scale brightness variations that may be associated with localized magnetic activity. In the Sun $<1\%$ of the surface is covered by active regions, while in more active stars, such as AB Dor, $\sim 8.5\%$ of the stellar surface may be covered by active regions, some of them quite large (Donati et al. 2003). In Figure 2 we show a simple limb-brightened profile in panel (a). In the other panels, $\sim 1\%$ of the stellar surface is brighter than the average stellar level by a factor of (b) 2, (c) 5, and (d) 10. Such a feature could be discernible in spectra obtained by *FUSE*.

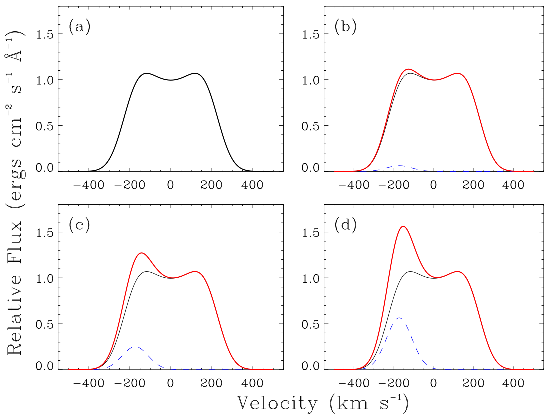

Figure 2. A model of a limb-brightened line profile of a star with a $v \sin i \sim 210$ km s^{-1} is shown in panel (a). Subsequent panels show the effect on the line profile of a small bright region, approximately 1% of the stellar surface, present on the face of the stellar disk. In panel (b) the small bright region is 2 times brighter than the quiescent stellar levels, for panel (c) it is 5 times brighter, and panel (d) it is 10 times brighter. The basic limb-brightened line profile is present in all panels, along with the small bright region contribution (dashed line), and the resulting total line profile.

3. Two Epochs of *FUSE* Observations

We obtained *FUSE* observations of Altair on two separate occasions: Epoch 1 on 14 September 2001 for 4.2 ksec, and Epoch 2 on 13 May 2004 for 26.9 ksec (9.8 ksec of which was taken during orbital "night-time"). During Epoch 2 we hoped to monitor the star over at least one stellar rotation, in order to search for transition line profile variations. In Figure 3, the C III and O VI lines for the two epochs are compared. The O VI lines agree very well, with only a slight discrepancy near the blue peak. The C III lines, however, are significantly different, but due to an instrumental effect rather than an intrinsic long-term stellar variation. Ake et al. (2000) found that scattered solar light contaminated the C III region in a *FUSE* observation of AB Dor. Unfortunately, the Epoch 1 observations were taken in HISTOGRAM mode, where the timing information for each photon was discarded onboard the spacecraft. Therefore, we are unable to separate "night-time" photons from "day-time" photons. For the Epoch 2 observation, taken in TIME-TAG mode, we are able to isolate the "night-time" photons, and therefore eliminate any scattered solar contamination. Therefore, although the C III line is the strongest stellar emission line in the spectrum, its effective integration time is cut roughly in half, and the signal-to-noise (S/N) is slightly worse compared to O VI. (Note the local interstellar medium (LISM) absorption line is clearly visible in the Epoch 2 observation).

4. Simple Limb-Brightening Law Fits

We fit a simple $1/\mu$, where $\mu = \cos\theta$, limb-brightening law to the strong emission lines C III and O VI of both epochs in Figure 4. We do not include the C III line of Epoch 1, due to the contamination of scattered solar light. The fits assume the emission is optically thin (perhaps not appropriate for C III), and from the slope and extent of the emission at the very edges, we are able to fit the effective line width and total $v \sin i$. The effective line width is assumed to be identical for all stellar rotational zones. After removing the contribution of the thermal component,

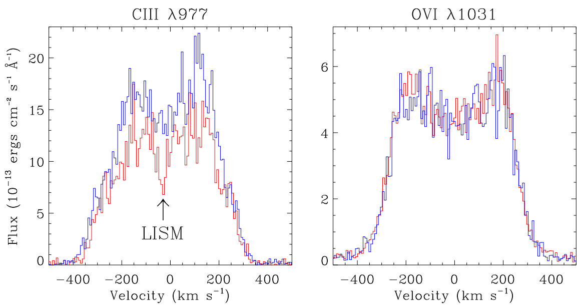

Figure 3. Comparison of the Epoch 1 (dark blue histogram) and Epoch 2 (light red histogram) line profiles of C III and O VI. The sharp absorption line in the Epoch 2 C III profile is consistent with the absorption expected from the local interstellar medium (LISM). The O VI lines agree fairly well, while the discrepancy between the C III lines can be explained by scattered solar light contamination during Epoch 1.

the nonthermal line width is ~ 50 km s^{-1}, in agreement with other late-type stars (Redfield et al. 2002, Wood et al. 1997). The effective $v \sin i$ is 230 km s^{-1} for C III and 250 km s^{-1} for O VI, slightly higher than the value obtained by optical interferometry 210 $\pm$ 13 km s^{-1} (van Belle et al. 2001) and an optical line profile analysis 227 $\pm$ 11 km s^{-1} (Reiners & Royer 2004), but perhaps consistent with extended high temperature emission beyond the photosphere. This simple limb-brightening model does very well in fitting the O VI profile, and marginally well in fitting the C III profile, potentially because C III is optically thick.

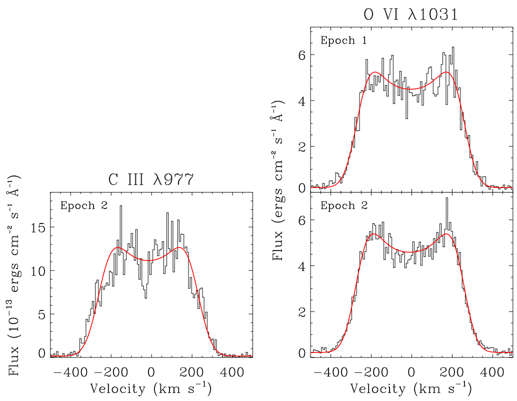

Figure 4. Fits to the limb-brightened profiles of C III and O VI. A simple limb-brightening law ($1/\mu$) is assumed, and is moderately successful at fitting the data. Although, deviations are evident, particularly in the wings of the C III line. These simple fits to each individual epoch, will be the basis for searching for short-term line profile variations.

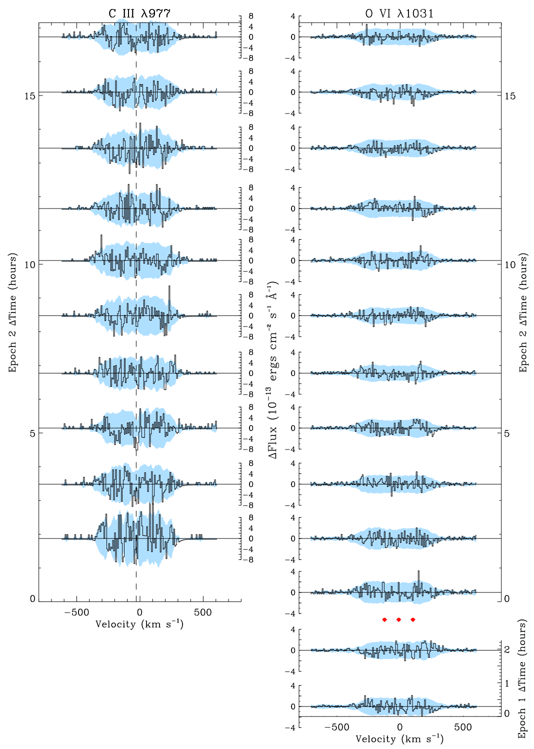

Figure 5. Difference between the simple limb-brightened profile fit of the entire observation (see Figure 4), and the observed line profile for each individual exposure (each approximately 1-2 ksec in duration). The C III residuals are not included for Epoch 1 because of the scattered solar light contamination. The LISM absorption is indicated by the dashed line, and is evident in each C III profile. The 1σ error bars are indicated by the shaded region. No obvious feature is observed to track across the stellar disk.

5. Searching for Line Profile Variations

Using the simple limb-brightened profiles, we search for short-term variations in the line profiles of C III and O VI. Figure 5 shows the difference between the simple limb-brightened profile shown in Figure 4, which was a fit to the entire observation, and each individual exposure. The Epoch 2 observation is divided into 11 different exposures (10 for C III). The light shading indicates the 1-sigma error bars. The Epoch 1 observation is divided into 2 individual exposures for O VI. The lower S/N of the C III line is immediately obvious (note the change in the ΔFlux scale). No strong singular emission variation is detected, and therefore if an individual active region (~ 1% of the stellar surface in size) is present on the stellar surface, then it is $\lesssim 2.8$ times brighter than a comparable quiet region.

The LISM absorption feature is seen in each exposure of the C III profile.

6. Fitting Arbitrary Limb-Brightening Functions

Instead of assuming the standard $1/\mu$ limb-brightening law, we explicitly fit the line profile to obtain the brightening function directly. In Figure 6, we compare an arbitrary limb-brightening dependence (light lines) with the standard $1/\mu$ law (dark lines). The resulting fit to the line profile is shown in the plots on the right. Deviations from the simple $1/\mu$ law are clear, particularly in the C III line profile. However, no corresponding discrepancy is measured in the Epoch 2 O VI line profile.

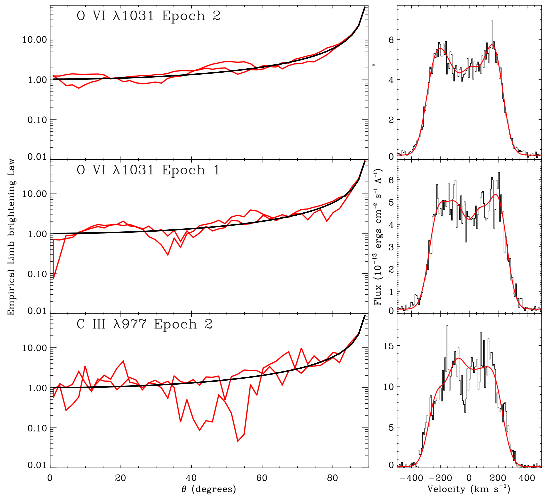

Figure 6. Free fits to the limb-brightening law. The simple $1/\mu$ law is shown as the dark line, while the fit to each side of the line is shown by the lighter lines. The fits agree fairly well with the standard $1/\mu$ limb-brightening law. The resulting line profiles are also shown on the right.

7. Conclusions

The unique "horned" emission line profiles discussed here, provide an opportunity to investigate heating mechanisms and other phenomena associated with the transition regions of stellar atmospheres. Limb-brightened profiles observed in UV spectra of the Sun have provided valuable insight into the structure of the solar atmosphere. We present the first evidence for limb-brightening in a UV emission line, for a star other than the Sun. A full discussion and analysis will be presented in a forthcoming paper (Redfield et al. 2004, in preparation). This data is not only an aid to understanding the large-scale structure of Altair's stellar atmosphere, but can also be used to place limits on the physical characteristics of possible localized transition region structures crossing the stellar disk.

Acknowledgements

This research was supported by NASA grant NNG04GM53G and is based on observations made with the NASA-CNES-CSA *Far Ultraviolet Spectroscopic Explorer* under Guest Investigator program D099. *FUSE* is operated for NASA by the Johns Hopkins University, under NASA contract NAS5-32985.

References

Ake, T.B., Dupree, A.K., Young, P.R., Linsky, J.L., Malina, R.F., Griffiths, N.W., Siegmund, O.H.W., & Woodgate, B.E. 2000, ApJ, 538, L87

Crane, P.C., Floyd, L.E., Cook, J.W., Herring, L.C., Avrett, E.H., & Prinz, D.K. 2004, A&A, 419, 735

Donati, J.-F., Collier Cameron, A., Petit, P. 2003, MNRAS, 345, 1145

Doschek, G.A., Feldman, U., & Tousey, R. 1975, ApJ, 202, L151

Hatzes, A.P. 1996, in IAU Symp. 176, Stellar Surface Structure, ed. K.G. Strassmeier & J.L. Linsky (Dordrecht: Kluwer), 305

Huenemoerder, D.P., Ramsey, L.W., Buzasi, D.L., & Nations, H.L. 1993, ApJ, 404, 316

Redfield, S., Ayres, T.R., Linsky, J.L., Ake, T.B., Dupree, A.K., Robinson, R.D., & Young, P.R. 2003, ApJ, 585, 993

Redfield, S., Linsky, J.L., Ake, T.B., Ayres, T.R., Dupree, A.K., Robinson, R.D., Wood, B.E., & Young, P.R. 2002, ApJ, 581, 626

Reiners, A., & Royer, F. 2004, A&A, in press

Simon, T., Ayres, T.R., Redfield, S., & Linsky, J.L. 2002, ApJ, 579, 800

van Belle, G.T., Ciardi, D.R., Thompson, R.R., Akeson, R.L., & Lada, E.A. 2001, ApJ, 559, 1155

Wilhelm, K., et al. 1998, A&A, 334, 685

Wood, B.E., Linsky, J.L., & Ayres, T.R. 1997, ApJ, 478, 745

Zirin, H. 1975, ApJ, 199, L63